Natural Science Report, Ochanomizu University, Vol. 6, No. 2, 1956
お茶の水女子大学 自然科学報告 第6巻 第2号

On the Structure of the Atmospheric Turbulence Near the Ground V[1)]

Jiro Sakagami (坂上治郎)

Department of Physics, Faculty of Science,
Ochanomizu University, Tokyo.

Introduction

The author has found out eddies as elements of the atmospheric turbulence, and investigated their structures, dynamical quantities and time variations, by a method of analysis[2)] which is based upon examination into characteristic features of records obtained by simultaneous observations of several hot-wire anemometers, or examination into contours of equi-deflecting angles observed by a number of special small wind-vanes distributed over a certain area[(1)]. In 1950, using the author's observational data, Ogawara analysed the eddies statistically[(2)]. At that time he used two kinds of models: A) one of which was that the eddy is circular and isolated and its velocity distribution is sinusoidal within the circle and is equal to zero outside of it, and B) the other one was that positive and negative eddies are arranged alternatively and are in contact with each other. Then he calculated cross-wind (y-ward) correlation and comparing with the observational results, he concluded that the model A was not adoptable, because the lowest minimum of the correlation curve was still higher than the minimum obtained by the observations.

In oscillograms of simultaneous observations of several hot-wire anemometers, we have noticed that there are special patterns which show the existence of the eddies appear at intervals and in somewhat lumpy forms. So it seems to us that the model A is more natural than the model B; furthermore Ogawara's calculation needs some corrections and the corrected results lead the conclusion that the model A is not always to be abandoned[(3)].

Therefore, we intended to calculate the correlation by using the model which was adopted in the morphological analysis and to examine the justification of the model and the method of the analysis itself.

Turbulent velocity components

We choose x-axis along the mean wind direction, z-axis vertically

1) This work was carried under a Grant in Aid for Fundamental Scientific Research from the Ministry of Education.

2) We may call this analysis the 'morphological' analysis.

and y-axis perpendicularly to them. The turbulent velocity components are given by[3,4]

$$u'=-V_p y/R, \qquad v'=V_p x/R, \qquad \sqrt{x^2+y^2}\leq R \tag{1.1}$$

$$u'=-V_p Ry/(x^2+y^2), \quad v'=V_p Rx/(x^2+y^2), \quad \sqrt{x^2+y^2}\geq R \tag{1.2}$$

where R is the radius of the circular area in which the vorticity is constant, and V_p is the periphery velocity on the circle[4].

The oscillogram records the total velocity V,

$$V=\sqrt{(U+u')^2+v'^2+w'^2},$$

where U is the mean wind velocity, but, as u', v' and w' are small compared with U, we get

$$V\sim U+u',$$

so the deviations from the mean can be considered as u'.

Correlation function

Now we calculate the occurrence probability of the correlation at two points separated at a distance r along y-axis.

Introducing new variables $x/R=\xi$, $y/R=\eta$ and $r/R=\rho$, we define next functions:

$$i_1\equiv -V_p\eta \quad (\sqrt{\xi^2+\eta^2}\leq 1), \qquad i_2\equiv -V_p(\eta+\rho) \quad (\sqrt{\xi^2+(\eta+\rho)^2}\leq 1) \tag{2.1}$$

$$e_1\equiv -V_p\frac{\eta}{\xi^2+\eta^2} \quad (\sqrt{\xi^2+\eta^2}\geq 1), \quad e_2\equiv -V_p\frac{\eta+\rho}{\xi^2+(\eta+\rho)^2} \quad (\sqrt{\xi^2+(\eta+\rho)^2}\geq 1). \tag{2.2}$$

A) When ξ lies between ξ and $\xi+d\xi$, the occurrence probability $P(\xi, \rho)d\xi$ of the correlation between two points separated at a distance ρ along y-axis is given as follows:—

We must remark here that the integrals which appear in this calculation become infinite if they are extended over the whole domain. So we integrate them within the domain $-L\leq(x, y)\leq L$.

i) $\rho=0$

$$0\leq\xi\leq 1, \quad Q_1(\xi, 0)=\int_{-\lambda}^{\eta_1} e_1^2 d\eta+\int_{\eta_1}^{\eta_4} i_1^2 d\eta+\int_{\eta_4}^{\lambda} e_1^2 d\eta \tag{3.1}$$

$$1\leq\xi, \quad Q_2(\xi, 0)=\int_{-\lambda}^{\lambda} e_1^2 d\eta \tag{3.2}$$

3) The vertical component becomes negligible when the observation is made at a height more than 60 cm. from the ground[5].

4) This distribution is that of well-known 'circular vortex'.

ii) $\rho \leq 2$

$$0 \leq \xi \leq \xi_1 = \sqrt{1-\frac{\rho^2}{4}}$$

$$P_1(\xi, \rho) = \left\{\int_{-\lambda}^{\eta_1} e_1 e_2 d\eta + \int_{\eta_1}^{\eta_2} e_1 i_2 d\eta + \int_{\eta_2}^{\eta_3} i_1 i_2 d\eta + \int_{\eta_3}^{\eta_4} i_1 e_2 d\eta + \int_{\eta_4}^{\lambda-\rho} e_1 e_2 d\eta\right\} / Q_1(\xi, 0) \quad (4.1).$$

$$\xi_1 \leq \xi \leq 1$$

$$P_2(\xi, \rho) = \left\{\int_{-\lambda}^{\eta_1} e_1 e_2 d\eta + \int_{\eta_1}^{\eta_2'} e_1 i_2 d\eta + \int_{\eta_2'}^{\eta_2} e_1 e_2 d\eta + \int_{\eta_2}^{\eta_4} i_1 e_2 d\eta + \int_{\eta_4}^{\lambda-\rho} e_1 e_2 d\eta\right\} / Q_1(\xi, 0) \quad (4.2).$$

$$1 \leq \xi$$

$$P_3(\xi, \rho) = \int_{-\lambda}^{\lambda-\rho} e_1 e_2 d\eta / Q_2(\xi, 0) \quad (4.3).$$

iii) $\rho \geq 2$

$$0 \leq \xi \leq 1$$

$$P_4(\xi, \rho) = \left\{\int_{-\lambda}^{\eta_1} e_1 e_2 d\eta + \int_{\eta_1}^{\eta_2'} e_1 i_2 d\eta + \int_{\eta_2'}^{\eta_2} e_1 e_2 d\eta + \int_{\eta_2}^{\eta_4} i_1 e_2 d\eta + \int_{\eta_4}^{\lambda-\rho} e_1 e_2 d\eta\right\} / Q_1(\xi, 0) \quad (5.1).$$

$$1 \leq \xi$$

$$P_5(\xi, \rho) = \int_{-\lambda}^{\lambda-\rho} e_1 e_2 d\eta / Q_2(\xi, 0) \quad (5.2),$$

where

$$\eta_1 = -\sqrt{1-\xi^2} - \rho, \quad \eta_2 = -\sqrt{1-\xi^2},$$
$$\eta_3 = \sqrt{1-\xi^2} - \rho, \quad \eta_4 = \sqrt{1-\xi^2},$$
$$\eta_2' = \sqrt{1-\xi^2} - \rho \quad (= \eta_3) \quad (6)$$

(cf. Fig. 1[5]).

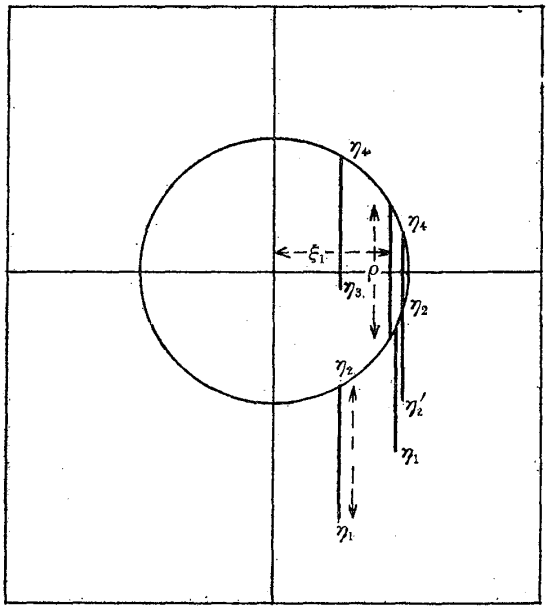

Fig. 1.

B) We calculate the mean values, referring to ξ, of these quantities. As $P_i(\xi, \rho)d\xi$ is even function of ξ, we obtain

$$\rho \leq 2$$

$$P(\rho) = \left\{\int_0^{\xi_1} P_1(\xi, \rho)d\xi + \int_{\xi_1}^{1} P_2(\xi, \rho)d\xi + \int_1^{\lambda} P_3(\xi, \rho)d\xi\right\} \Big/ \lambda \quad (7.1)$$

$$\rho \geq 2$$

$$P(\rho) = \left\{\int_0^{1} P_4(\xi, \rho)d\xi + \int_1^{\lambda} P_5(\xi, \rho)d\xi\right\} \Big/ \lambda, \quad (7.2)$$

5) The length of thick line is ρ.

where $\lambda=L/R$.

Considering the accuracy of record of hot-wire anemometer, it is diffiucult to discriminate the velocity smaller than 10 cm./sec. when the mean velocity is about 2~3 m/sec. If we denote the distance where u' becomes this critical value by y_0, and if we assume that V_p/U is 0.1 and U is 2 m/sec,

$$10 \geq |u'| = V_p R/y_0 = 0.1UR/y_0 = 20R/y_0 ,$$

so we get $y_0=2R$. Therefore we assume that $L=2R$, accordingly $\lambda=2$.

C) The terms in the functions $P_i(\xi, \rho)d\xi$'s are given explicitly in the next forms:—

1) $$\left(\int_{-\lambda}^{\eta_1}+\int_{\eta_4}^{\lambda-\rho}\right)(e_1e_2)d\eta = V_p^2\left(\int_{-\lambda}^{\eta_1}+\int_{\eta_4}^{\lambda-\rho}\right)\left(\frac{\eta(\eta+\rho)}{(\xi^2+\eta^2)\{\xi^2+(\eta+\rho)^2\}}\right)d\eta$$
$$= V_p^2\frac{1}{\rho(4\xi^2+\rho^2)}\left[(2\xi^2+\rho^2)\log\left\{(1+\rho^2+2\rho\sqrt{1-\xi^2})\frac{\xi^2+(\lambda-\rho)^2}{\xi^2+\lambda^2}\right\}\right.$$
$$\left.+2\rho\xi\left(\tan^{-1}\frac{\lambda-\rho}{\xi}+\tan^{-1}\frac{\lambda}{\xi}-\tan^{-1}\frac{\sqrt{1-\xi^2}}{\xi}-\tan^{-1}\frac{\sqrt{1-\xi^2}+\rho}{\xi}\right)\right] \tag{8.1}$$

2) $$\int_{\eta_1}^{\eta_2} e_1i_2d\eta = V_p^2\int_{\eta_1}^{\eta_2}\frac{\eta(\eta+\rho)}{\xi^2+\rho_2}d\eta = V_p^2\left[\rho-\frac{\rho}{2}\log(1+\rho^2+2\rho\sqrt{1-\xi^2})\right.$$
$$\left.+\xi\left(\tan^{-1}\frac{\sqrt{1-\xi^2}}{\xi}-\tan^{-1}\frac{\sqrt{1-\xi^2}+\rho}{\xi}\right)\right] \tag{8.2}$$

3) $$\int_{\eta_3}^{\eta_4} i_1e_2d\eta = V_p^2\int_{\eta_3}^{\eta_4}\frac{\eta(\eta+\rho)}{\xi^2+(\eta+\rho)^2}d\eta = V_p^2\left[\rho-\frac{\rho}{2}\log(1+\rho^2+2\rho\sqrt{1-\xi^2})\right.$$
$$\left.-\xi\left(\tan^{-1}\frac{\sqrt{1-\xi^2}+\rho}{\xi}-\tan^{-1}\frac{\sqrt{1-\xi^2}}{\xi}\right)\right] \tag{8.3}$$

4) $$\int_{\eta_2}^{\eta_3} i_1i_2d\eta = V_p^2\int_{\eta_2}^{\eta_3}\eta(\eta+\rho)d\eta = V_p^2(2\sqrt{1-\xi^2}-\rho)$$
$$\times\left[\frac{1}{3}(1-\xi^2-\rho\sqrt{1-\xi^2})-\frac{\rho}{6}\right] \tag{8.4}$$

5) $$\int_{\eta_1}^{\eta_2'} e_1i_2d\eta = V_p^2\int_{\eta_1}^{\eta_2'}\frac{\eta(\eta+\rho)}{\xi^2+\eta^2}d\eta = V_p^2\left[2\sqrt{1-\xi^2}+\frac{\rho}{2}\log\frac{\xi^2+(\sqrt{1-\xi^2}-\rho)^2}{\xi^2+(\sqrt{1-\xi^2}+\rho)^2}\right.$$
$$\left.-\xi\left(\tan^{-1}\frac{\sqrt{1-\xi^2}-\rho}{\xi}+\tan^{-1}\frac{\sqrt{1-\xi^2}+\rho}{\xi}\right)\right] \tag{8.5}$$

6) $$\int_{\eta_2}^{\eta_4} i_1e_2d\eta = V_p^2\int_{\eta_2}^{\eta_4}\frac{\eta(\eta+\rho)}{\xi^2+(\eta+\rho)^2}d\eta = V_p^2\left[2\sqrt{1-\xi^2}-\frac{\rho}{2}\log\frac{\xi^2+(\sqrt{1-\xi^2}+\rho)^2}{\xi^2+(\sqrt{1-\xi^2}-\rho)^2}\right.$$
$$\left.-\xi\left(\tan^{-1}\frac{\sqrt{1-\xi^2}+\rho}{\xi}+\tan^{-1}\frac{\sqrt{1-\xi^2}-\rho}{\xi}\right)\right] \tag{8.6}$$

$$7)\quad \left(\int_{-\lambda}^{\eta_1}+\int_{\eta_4}^{\lambda}\right)e_1^2d\eta=V_p^2\left(\int_{-\lambda}^{\eta_1}+\int_{\eta_4}^{\lambda}\right)\left(\frac{\eta^2}{(\xi^2+\eta^2)^2}\right)d\eta$$

$$=V_p^2\left[-\frac{1}{\xi}\left(\tan^{-1}\frac{\sqrt{1-\xi^2}}{\xi}-\tan^{-1}\frac{\lambda}{\xi}\right)+\sqrt{1-\xi^2}-\frac{\lambda}{\xi^2+\lambda^2}\right] \qquad (8.7)$$

$$8)\quad \int_{\eta_1}^{\eta_4}i_1^2d\eta=V_p^2\int_{\eta_1}^{\eta_4}\eta^2d\eta=V_p^2\frac{2}{3}(\sqrt{1-\xi^2})^3 \qquad (8.8)$$

$$9)\quad \int_{-\lambda}^{\lambda}e_1^2d\eta=V_p^2\int_{-\lambda}^{\lambda}\frac{\eta^2}{(\xi^2+\eta^2)^2}\,d\eta=V_p^2\left[\frac{1}{\xi}\tan^{-1}\frac{\lambda}{\xi}-\frac{\lambda}{\xi^2+\lambda^2}\right] \qquad (8.9)$$

D) We integrate the equations (7.1) and (7.2) numerically by the Gauss-Lobatto's method for $n=5$ and obtaine the curve given in Fig. 2.

The resulted curve decreases rapidly from its initial value 1 and, showing distinctly negative correlation, becomes minimum at $\rho=2$, i.e. at the distance corresponding the diameter of the eddy, then increases gradually and becomes zero at $\rho\geq 4$[6].

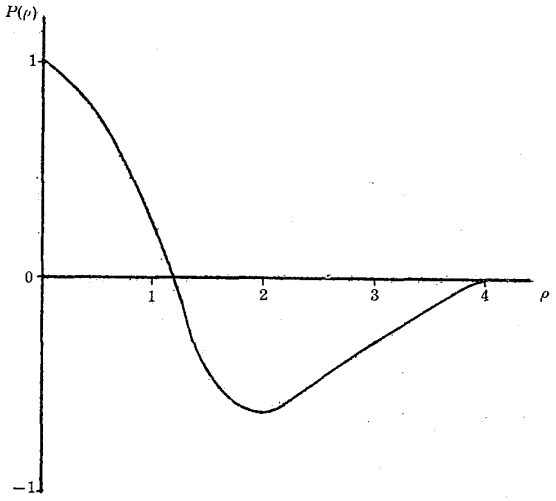

Fig. 2.

The effect of the size distribution

The eddies in the atmosphere are not uniform size and, even in crude approximation, we cannot neglect the size distribution. So we must consider its effect on the correlation. As a special case, we adopt

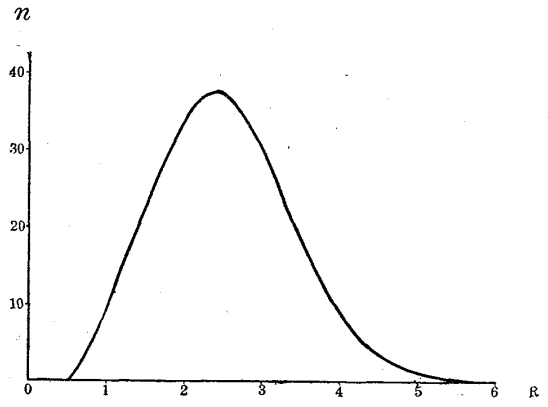

Fig. 3.

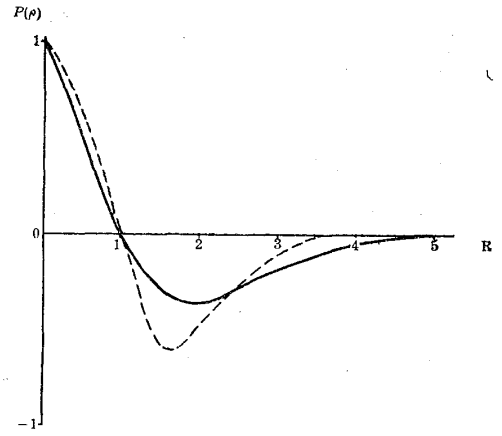

Fig. 4.

6) The is the result of that we assumed $\lambda=2$.

the size distribution given in Fig. 3, and we get the result shown in Fig. 4[7]; namely the distance at which the correlation attains minimum becomes larger than that corresponds to the mode of the size distribution and the depth of the minimum becomes shallower.

The effect of the passage of the eddy

The larger eddy spends more time than the smaller eddy when it passed the line on which the hot-wire anemometers are arranged, so when we calculate the correlation by measuring the records of oscillograms at a definite time interval, the probability to be measured becomes larger as the size of the eddy increases.

The time of passage τ is proportional to $R/U\Delta t$, where Δt is the time interval of measuring. The probability to be counted is proportional to τ, so we use τ as the 'duration factor' and mutiply this to the size distribution and then using this corrected distribution, we calculate the correlation.

Comparison with the observational data

The data of the observation are given in Table 1 and Figs. 5, 6, 7 and 8. Δt was 0.1 sec. and the number of measuring was 100, so the total observing time was 10 sec. The deviations of velocity at each position of hot wire anemometer from the mean taken by the data were used as u'. As we needed the size distribution, we used the results ob-

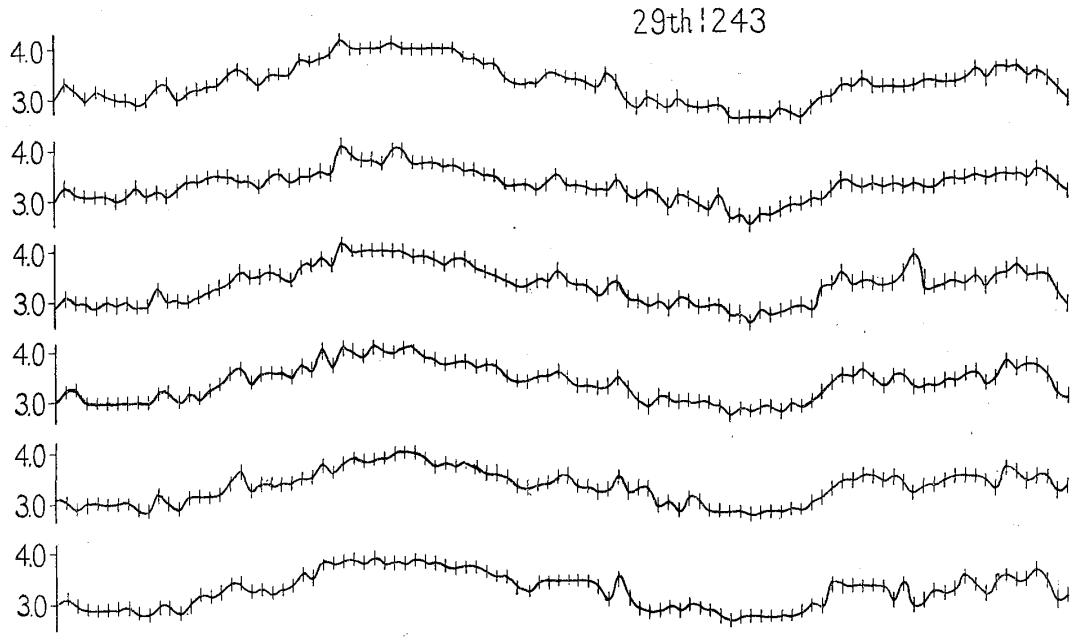

Fig. 5.

7) In this figure broken line shows the curve for uniform size and full line shows the result considered the size distribution.

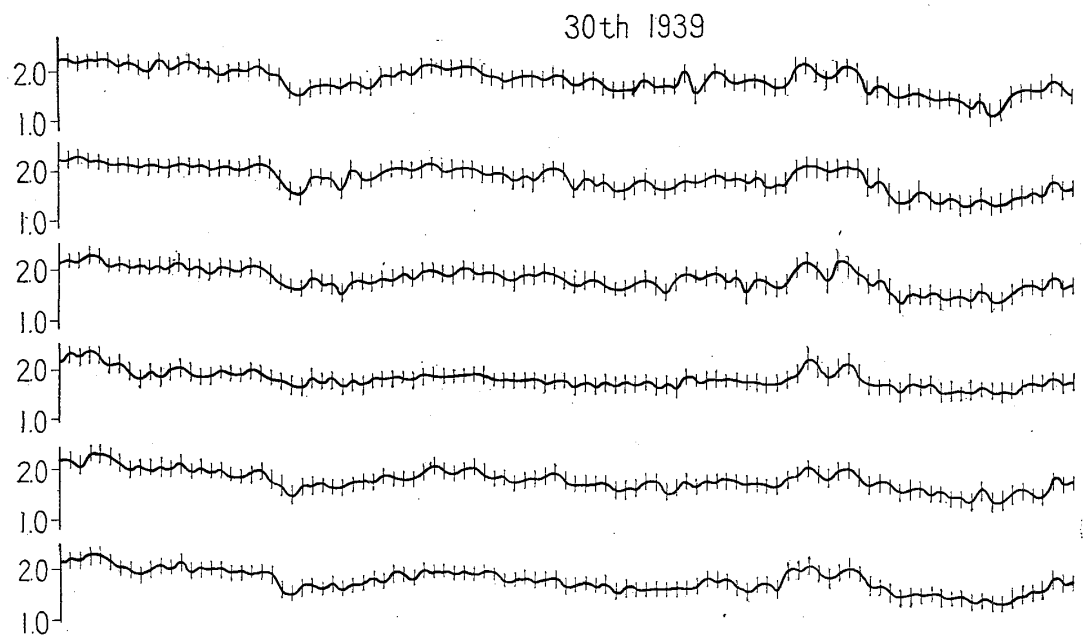

Fig. 6.

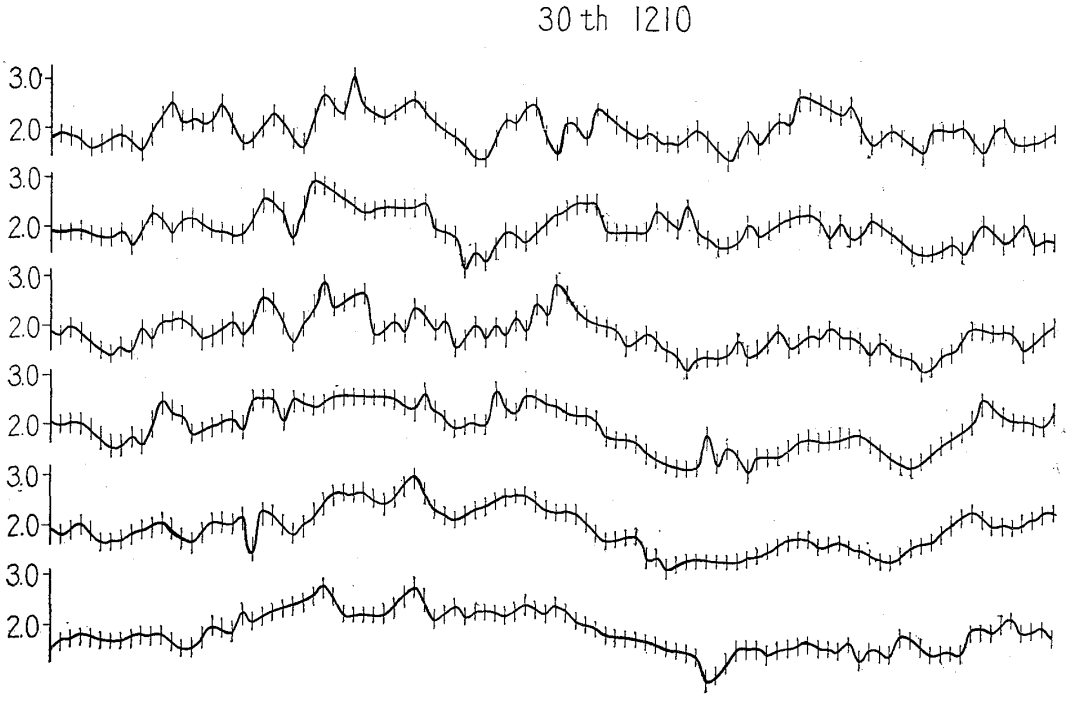

Fig. 7.

Table 1.

Location	Date	Interval of Hot-wire anemometers Δ (cm.)	Height H (m)	Mean Wind Velocity U (m/sec)
Chiba	29 1243	1.5	1	2.85
Chiba	30 1939	1.5	1	1.81
Chiba	30 1210	10	1	1.96
Nakano	31 0930	5	6	2.30

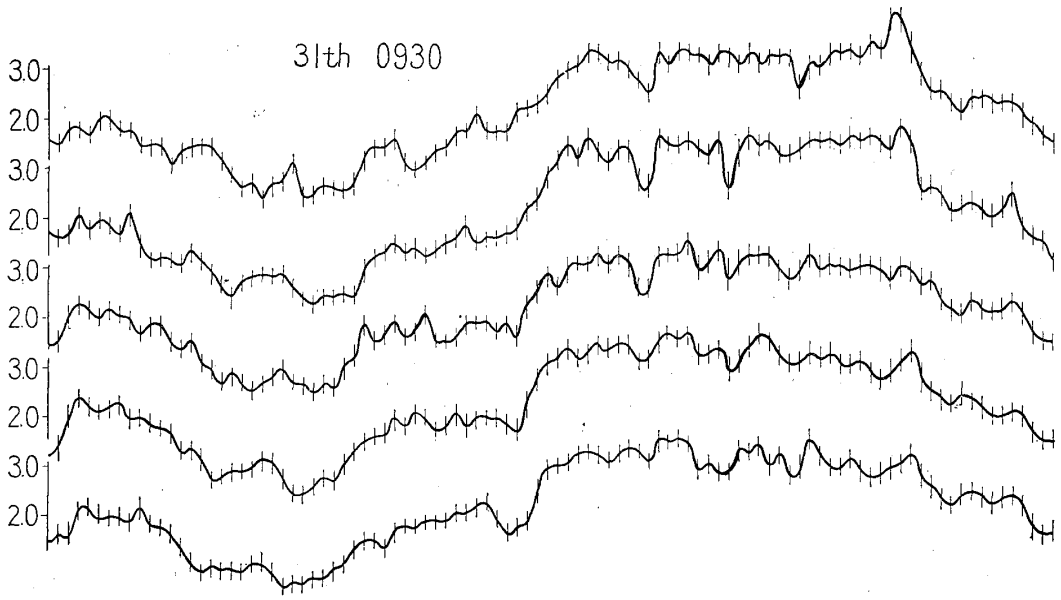

Fig. 8.

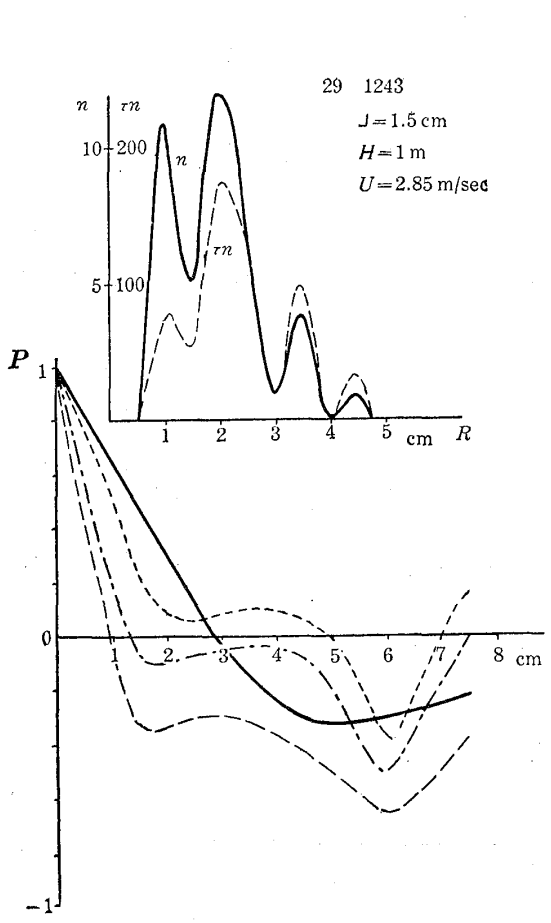

Fig. 9.

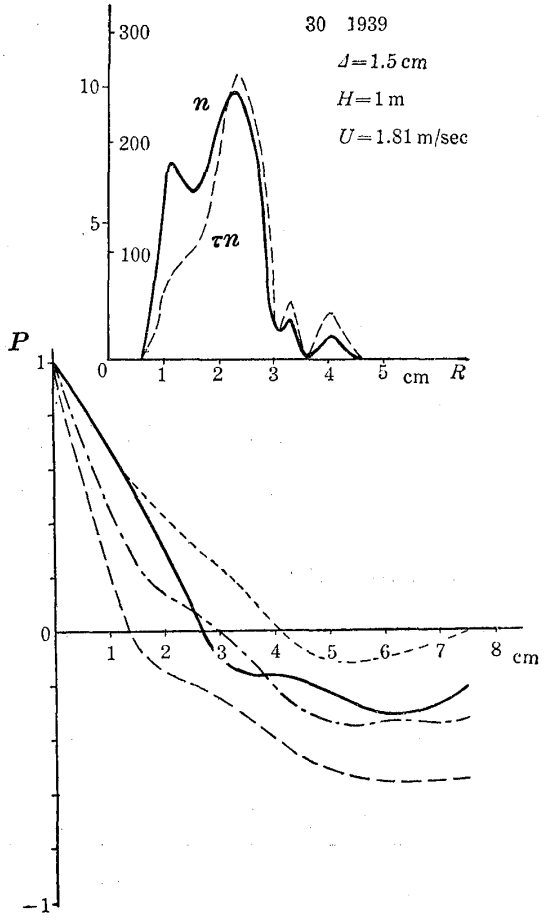

Fig. 10.

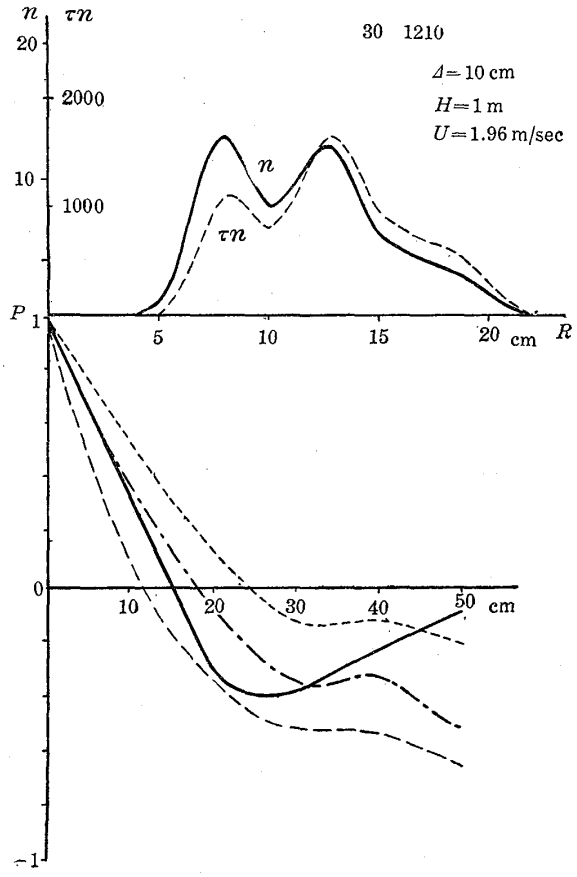

Fig. 11.

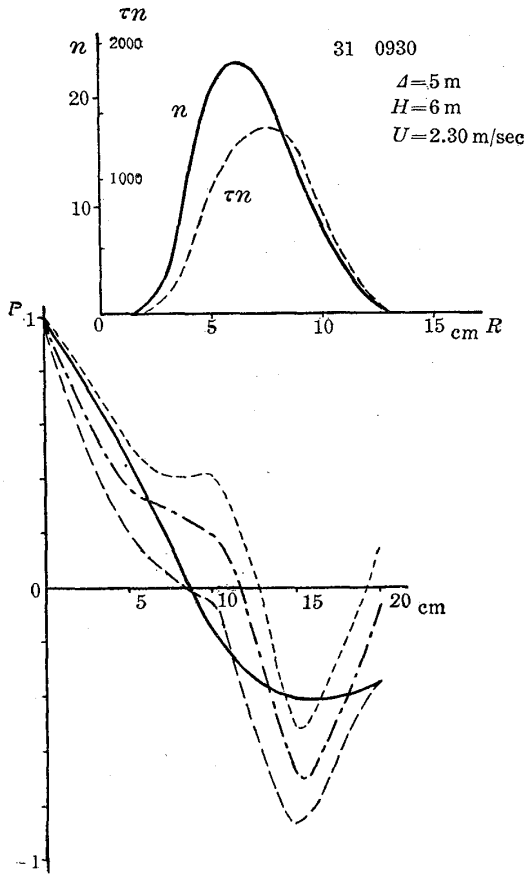

Fig. 12.

tained by the morphological analysis. The results are shown in Figs. 9, 10, 11 and 12[8]. The curves varies considerably even when the order of the positions of the hot-wires is reversed, so the agreement may be deemed passably good.

Consideration about the shape of the correlation curve

As we remarked already, the correlation curve decreases repidly from its initial value 1 and clearly show the negative correlation and then gradually tends to zero. The curve considered at present corresponds to the curve of the Eulerian g-function, but the negative portion of the latter is not so remarkable, because it must satisfy the equation $\int_0^\infty rg(r)dr=0$.

Some typical examples in which the velocity variations are only positive or negative (A) are shown in Fig. 13 and those in which the positive and the negative variations are always combined together (B) are shown in Fig. 14.

8) In these figures full lines indicate the calculated curves, chain lines the observed curves and dotted lines the 98% confidence limits.

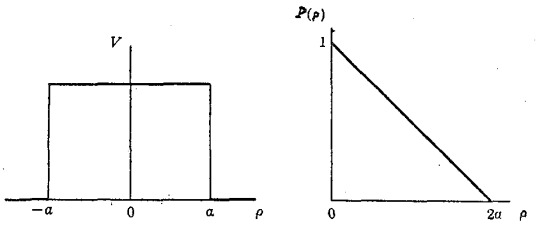

Fig. 13. (a)

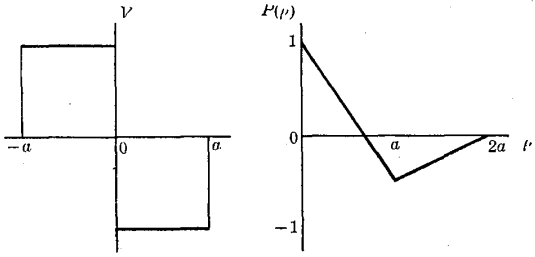

Fig. 14 (a)

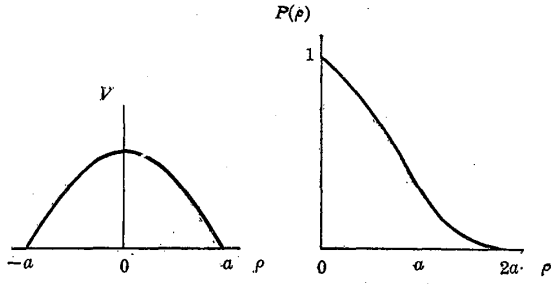

Fig. 13. (b)

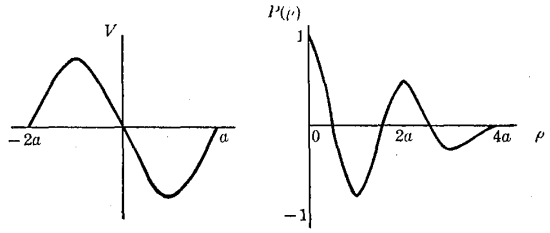

Fig. 14. (b)

We can see that the cases A do not show any part of negative correlation but the cases B clearly show the negative parts. Though the shapes of g-function obtained by wind-tunnel experiments may belong to the cases A, those obtained by the observations in the atmosphere belong to the cases B, even the interval of hot-wire anemometers and the wind velocity are of the same order in both observations. So we can conclude that the elements of turbulence in the atmosphere have the structures in which the positive and the negative variations of wind velocity connected each other, but in the wind-tunnel, though the positive or negative variations occur at random, each of them has little connections and behaves like a pulse.

In the wind-tunnel vortices are generated by grids or honeycombs and then deform into turbulence. They are generated much more densely than in the atmosphere, so the destructive effect of each vortex owing to the mutual interferences is much more intense than in the another. This may be the reason that there is a distinct difference between both cases.

Conclusion

1) The assumption of 'circular vortex' which has been adopted in the morphological analysis is also appropriate when it is used in the statistical analysis[9], and as the results considering the size distributions obtained by the former analysis agree fairly good with the observations, the analysis itself can be judged as is appropriate.

2) Though the morphological method is very laborious, it can find

9) The assumption has been verified by the morphological analysis[6].

out each element of the turbulence and measure its size, vorticity and life time, and can examine it intrinsic structure and three dimensional one. This is a characteristic compared with the statistical method.

3) The turbulence in the atmosphere differs essentially from that in the wind-tunnel and the structure, in which the positive and the negative velocity variations are combined each other, cannot be neglected in the former.

4) The cause of this difference may be the difference of destructive effects owing to the space density of vortices between both cases.

To carry out this research many assistances were offered by Misses M. Matsuda, K. Araki and M. Iwasaki. The author wants to express his deepest thanks to these persons.

Literature

(1) Sakagami J. Natural Science Reports, Ochanomizu Univ. **1**; (1950) 40; **2** (1951) 52; **4** (1953) 201; Proc. 1st Japan Nat. Congr, App. Mech. (1951) 475.
(2) Ogawara M. Geophys. Mag. **21** (1950) 226.
(3) Ogawara M. Geophys. Mag. **27** (1956) 343.
(4) cf. (1)
(5) Sakagami J. Natural Science Reports, Ochanomizu Univ. **2** (1951) 52.
(6) Sakagami J. ibid. **1** (1950) 40; **2** (1951) 52.

(*Received Jan. 31, 1956*)